International Journal of Solids and Structures 46 (2009) 4313–4321

Contents lists available at ScienceDirect

International Journal of Solids and Structures

journal homepage: www.elsevier.com/locate/ijsolstr

Constitutive equations for 0-3 polarized PLZT actuators

Quantian Luo, Liyong Tong *

School of Aerospace, Mechanical and Mechatronic Engineering, The University of Sydney, NSW 2006, Australia

ARTICLE INFO

Article history:
Received 1 April 2009
Received in revised form 22 July 2009
Available online 26 August 2009

Keywords:
PLZT actuator
Photostriction
Strain variation
Nonlinearity
Constitutive equation

ABSTRACT

This article presents constitutive equations of transparent lead lanthanum zirconate titanate (PLZT) materials poling along thickness direction or with 0-3 polarization. Discussed first are the Beer's law of light transmission in transparent solid and the photovoltaic current density in PLZT materials. Formulas for field strength and electrical potential between two electrodes of a PLZT wafer are then derived from the basic photovoltaic equations. By superposing the photovoltaic and the converse piezoelectric effects, we formulate a novel expression for photo-induced strain that is nonlinearly dependent of incident light intensity and varies with light penetration depth in through-thickness direction. On the basis of the derived photo-induced strain, linear and nonlinear constitutive equations of 0-3 polarized PLZT actuators are formulated. The present model is validated by using the available experimental data in the literature. By using the present model with an exponential variation of strain through the thickness, closed-form solutions for the equivalent loads acting on a PLZT unimorph, bimorph and intelligent beam are obtained and then compared with numerical results available in the literature.

1. Introduction

Optical actuators have received considerable attention in recent years as they have found various applications in micro-electro/opto-mechanical system (MEMS/MOMS), ultrahigh vacuum and space technology. In an optical actuator, mechanical strain is induced by light illumination, which is referred to as photostriction. Photostrictive phenomena have been found in many materials, e.g., semiconductors (Figielski, 1961; Gauster and Habing, 1967), polymers (Eisenbach, 1980; Charra et al., 1993; Yu et al., 2003; Camacho-Lopez et al., 2004) and ferroelectric ceramics (Fridkin, 1979; Brody, 1983; Poosanaas-Burke et al., 1998; Ichiki et al., 2005). When light illuminates on a semiconductor, it generates free charge carriers due to absorption of photons, which results in mechanical deformation. Light illumination on polymeric materials with photo-responsive molecules produces mechanical deformation as a result of the reversible *trans-to-cis* transformation. The photo-induced strain in PbLaZrTi (PLZT) is a superposition of photovoltaic and converse piezoelectric effects. The light illumination also causes solid temperature variation giving rise to thermal expansion. It must be noted that the photostrictive effect is different from thermal dilatation owing to the temperature elevation.

Of these materials, PLZT ceramic is one of the most promising photostrictive materials as it has a high piezoelectric coefficient and is easy to fabricate. When near ultraviolet light illuminates on polarized PLZT materials, an electrical field is generated along spontaneous polarization direction due to the photovoltaic effect, and then mechanical strain is induced owing to the converse piezoelectric effect. The photovoltaic effect occurring within PLZT materials is considered to be an optical property of the material itself. The photovoltaic effect shows its merits in a number of aspects: (1) high electrical output voltage, (2) transducer from optical energy to electrical energy, (3) wireless energy transfer, (4) noise elimination vibration control, and (5) remote control. These characteristics are useful in MEMS and MOMS (Poosanaas-Burke et al., 1998; Ichiki et al., 2005).

The polarization is an essential concept in any phenomenological description of ferroelectric materials (Resta and Vanderbilt, 2007). The anomalous photovoltaic effect in PLZT materials is observed only in the direction of spontaneous polarization of ferroelectric materials. There are mainly two polarizing schemes for PLZT wafers (Ichiki et al., 2004; Leng et al., 2006), namely, poling in 0-1 (length) or 0-3 (thickness) direction, as shown in Fig. 1(a) and (b).

When a PLZT wafer with 0-1 polarization is illuminated by uniform ultraviolet light on surface in Fig. 1(a), an electrical field E_{11} is generated, and the photo-induced strain ε_{11} causes the PLZT wafer to deform in extension, as shown in Fig. 2(a). Photovoltaic mechanism and application of this type of PLZT actuator have been studied by some authors (Uchino et al., 1985; Fukuda et al., 1995; Poosanaas-Burke et al., 2000; Shih et al., 2005; Sun and Tong, 2007).

Recently, PLZT with 0-3 polarization shown in Fig. 1(b) has drawn much attention (Ichiki et al., 2005; Qin et al., 2007) since it is easier to fabricate in MEMS and MOMS applications and the

* Corresponding author. Tel.: +61 2 93516949; fax: +61 2 93514841.
E-mail address: ltong@aeromech.usyd.edu.au (L. Tong).

0020-7683/$ - see front matter © 2009 Elsevier Ltd. All rights reserved.
doi:10.1016/j.ijsolstr.2009.08.014

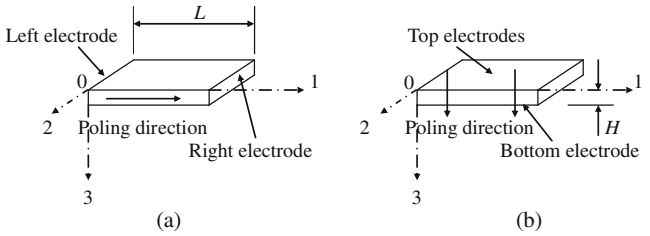

Fig. 1. Polarization orientation in a PLZT wafer: (a) electrically poled along length direction or 0-1 polarization and (b) electrically poled along thickness direction or 0-3 polarization.

applied voltage for polarization is considerably reduced. In this type of PLZT wafer, one electrode must be transparent so that light can penetrate the irradiating surface. The transparent electrode can be fabricated by sputtering Indium Tin Oxide (ITO) on the irradiating surface (Ichiki et al., 2005; Leng et al., 2006; Qin et al., 2007).

When light illuminates on a PLZT wafer with 0-3 polarization of Fig. 1(b), an electrical field E_{33} is produced and the photo-induced strain ε_{11} in this type of PLZT wafer create bending as illustrated in Fig. 2(b). This paper aims to develop linear and nonlinear constitutive equations of a PLZT wafer with 0-3 polarization. Novel formulation for the photo-induced strain will be derived and their applications will be discussed.

2. Phenomenological modeling of PLZT actuators, novel formulation of photo-induced strain

Photostriction of PLZT ceramics is a superposition of photovoltaic and converse piezoelectric effects, but the origin of photovoltaic effect in PLZT is not clear. To effectively utilize photostriction, several models have been proposed to depict photovoltaic mechanism in PLZT (Fridkin, 1979; Nonaka et al., 1995; Poosanaas-Burke et al., 2000; Qin et al., 2007). In this paper, we will develop phenomenological model for PLZT wafers with 0-3 polarization.

2.1. Basic photovoltaic equations, conductivity, current density and field strength

When illuminated by near ultraviolet light, PLZT materials will absorb photons and generate free charge carriers (Piprek, 2003; Yao et al., 2005). The continuity conditions of charge carrier currents are given by (Piprek, 2003):

$$q\frac{\partial n}{\partial t} = \nabla \cdot \{\boldsymbol{J}_n\} - q(R-G) \tag{1}$$

$$q\frac{\partial p}{\partial t} = -\nabla \cdot \{\boldsymbol{J}_p\} - q(R-G) \tag{2}$$

where t is time; q is the electron charge quantity, ∇ is the Laplace operator; $\{\boldsymbol{J}_n\}$ and $\{\boldsymbol{J}_p\}$ denote electron and hole current densities; G and R are the electron-hole pair generation and recombination rates; n and p represent electron and hole concentrations. When $\{\boldsymbol{J}_n\}$ and $\{\boldsymbol{J}_p\}$ are determined from Eqs. (1) and (2), and their superposition gives the photovoltaic current density (Yao et al., 2005).

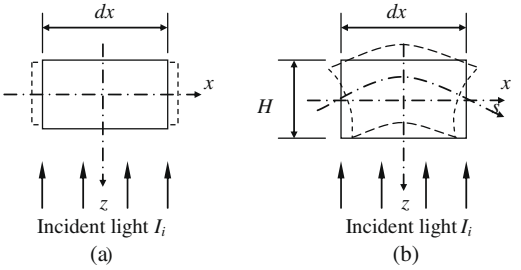

Fig. 2. Photo-induced deformation: (a) a PLZT wafer poled along length direction or 0-1 polarization and (b) a PLZT wafer poled along thickness direction or 0-3 polarization.

When light illuminates on surface of PLZT materials, the photovoltaic current density can be defined by (Fridkin, 1979):

$$\{\boldsymbol{J}_{ph}\}_{3\times1} = \alpha\alpha_s I_i e^{-\alpha z_d}\{\boldsymbol{k}\}_{3\times1} = \alpha I_o e^{-\alpha z_d}\{\boldsymbol{k}\}_{3\times1} \tag{3}$$

where $\{\boldsymbol{J}_{ph}\}_{3\times1} = \{J_{11}, J_{22}, J_{33}\}$ is the photocurrent density vector; α is the light absorption coefficient; α_s is the surface transmittance; I_i is the incident light intensity; $I_o(=\alpha_s I_i)$ is the light intensity beneath the illumination surface; and $\{\boldsymbol{k}\}_{3\times1} = \{k_1, k_2, k_3\}$ is a vector of the photocurrent density coefficient.

The electrical conductivity of PLZT materials can be defined as the sum of dark and photo conductivities (Fridkin, 1979):

$$[\boldsymbol{\kappa}]_{3\times3} = [\boldsymbol{\kappa}_d]_{3\times3} + [\boldsymbol{\kappa}_{ph}]_{3\times3} I_o e^{-\alpha z_d} \tag{4}$$

The relationship of current density and electrical field strength is given by (Saslow, 2002):

$$\{\boldsymbol{J}_{ph}\}_{3\times1} = [\boldsymbol{\kappa}]_{3\times3}\{\boldsymbol{E}_{ph}\}_{3\times1} \tag{5}$$

where $[\boldsymbol{\kappa}]_{3\times3} = \mathrm{diag}[\kappa, \kappa, \kappa]$, $[\boldsymbol{\kappa}_d]_{3\times3} = \mathrm{diag}[\kappa_d, \kappa_d, \kappa_d]$ and $[\boldsymbol{\kappa}_{ph}]_{3\times3} = \mathrm{diag}[\kappa_{ph}, \kappa_{ph}, \kappa_{ph}]$ for electrically isotropic materials; and $\{\boldsymbol{E}_{ph}\}_{3\times1} = \{E_{11}, E_{22}, E_{33}\}$ is the field strength vector.

It is known that the photo-induced field strength occurs along the poling direction of PLZT materials and two polarization orientations are practically used. Photovoltaic current and voltage in a PLZT wafer with 0-1 polarization were studied by Fukuda et al. (1995), Shih and Tzou (2000) and Poosanaas-Burke et al. (1998, 2000). A phenomenological model of PLZT materials with 0-3 polarization will be developed here based on the above equations.

2.2. Photocurrent continuity model of the photovoltaic effect, the converse piezoelectric effect and photo-induced strain

When a 0-3 polarized PLZT wafer is illuminated by near-violet light, photovoltage and photocurrent in the two opposite thickness directions are not symmetric (Fridkin et al., 1981; Qin et al., 2007). The Schottky barrier at the interface with the bottom electrode is different from that with the top one as their processing histories are different. Using Eqs. (3)–(5), the photo-induced field strength at z_d of the 0-3 polarized PLZT wafer can be derived as:

$$E_{33} = \frac{k_3\alpha I_o e^{-\alpha z_d}}{\kappa_d + \kappa_{ph} I_o e^{-\alpha z_d}} \tag{6}$$

where z_d is a distance measured from the light irradiation surface and denotes the light penetration depth. The electrical potential difference in a layer with thickness of (dz_d) at z_d can be derived in light of the basic relation of voltage and field strength, and is given by:

$$dV_{33} = E_{33}dz_d = \frac{k_3\alpha I_o e^{-\alpha z_d}}{\kappa_d + \kappa_{ph} I_o e^{-\alpha z_d}}dz_d \tag{7}$$

The voltage between the bottom and top electrodes can then be obtained by integrating equation (7) in $0 \leqslant z_d \leqslant H$:

$$V_{33} = \frac{k_3}{\kappa_{ph}}\ln\frac{\kappa_d + \kappa_{ph} I_o}{\kappa_d + \kappa_{ph} I_o e^{-\alpha H}} \tag{8}$$

where H is the wafer thickness.

By superposing the photovoltaic and the converse piezoelectric effects, the following novel photo-induced strain in a PLZT wafer with 0-3 polarization can be obtained:

$$\varepsilon_{ii} = \frac{d_{3i}k_3\alpha I_o e^{-\alpha z_d}}{\kappa_d + \kappa_{ph} I_o e^{-\alpha z_d}} \quad (i = 1, 2, 3) \tag{9}$$

where d_{3i} $(i = 1,2,3)$ are the coupling piezoelectric constants. It is seen from Eq. (9) that the photo-induced strain is nonlinearly related to the incident light intensity. The strain variation with the light penetrating depth in Eq. (9) will cause the PLZT wafer to deform in bending.

Poosanaas-Burke et al. (1998) investigated photovoltaic current and voltage of 0-1 polarized PLZT ceramics. The photo-induced strain and applications of a 0-1 polarized wafer have been studied by a number of authors, e.g., Uchino et al. (1985), Fukuda et al. (1995) and Shih et al. (2005). For a 0-3 polarized PLZT wafer, Ichiki et al. (2004, 2005) measured photovoltaic currents and voltages, and then fitted using the least square technique. Qin et al. (2007) studied photocurrents of 0-3 polarized wafers. A voltage between the top and bottom electrodes of a 0-3 polarized PLZT ceramics is explicitly expressed in Eq. (8) and the photo-strain is given in Eq. (9). To our best knowledge, Eqs. (6)–(9) are not available in open publications.

Eqs. (6)–(8) are derived from the basic photovoltaic equations, which reflect electrical performance. Eq. (9) is directly obtained by superposing the converse piezoelectric effect of PLZT materials. It indicates that the photo-induced strain nonlinearly depends on the light intensity and varies with light penetration depth nonexponentially. This photo-induced strain in 0-3 polarized PLZT actuators is different from that in PLZT actuators with 0-1 polarization, electrically-induced strain in PZT materials and the thermal expansion as the strains in these cases are uniform through the thickness normally. It is also different from the photo-induced strain in elastomer (Warner and Mahadevan, 2004) and in silicon (Guo et al., 2007). In the investigation of Warner and Mahadevan (2004) or Guo et al. (2007), the photo-induced strain linearly depends on the light intensity and exponentially decreases with the light penetration depth when the light intensity attenuates by Beer's law.

When $(\kappa_{ph} I_o/\kappa_d) \ll 1$, photo-induced field strength, voltage and strain are simplified as:

$$E_{33} = \frac{k_3 \alpha I_o e^{-\alpha z_d}}{\kappa_d}; \quad V_{33} = \frac{k_3 I_o}{\kappa_d}(1 - e^{-\alpha H});$$
$$\varepsilon_{ii} = \frac{d_{3i} k_3 \alpha I_o e^{-\alpha z_d}}{\kappa_d} \quad (i = 1,2,3) \tag{10}$$

In this case, the photo-induced strain decreases with the light penetration depth exponentially, which is the same as that discussed in Warner and Mahadevan (2004), Guo et al. (2007) and Luo and Tong (2009).

To apply Eq. (9) or Eq. (10) to MEMS/MOMS and intelligent structures, parameters d_{3i} $(i = 1,2,3)$, $\kappa_d, \kappa_{ph}, \alpha, \alpha_s$ and k_3 need to be determined by experiment. PLZT 3/52/48 is one of the most popular PLZT materials. Table 1 lists some values of these parameters of PLZT 3/52/48 and their sources.

In light of the continuity condition of photocurrent, photocurrent i_{33} will flow constantly along thickness direction in a PLZT wafer with 0-3 polarization. Based on Eqs. (1) and (2), spatial distributions of charge carries in this type of PLZT wafer can be solved for the prescribed boundary conditions when $(\partial n/\partial t) = 0$ and $(\partial p/\partial t) = 0$. In this steady state, the photo-induced charge carrier densities $n(z_d)$ and $p(z_d)$ have been found to decrease with the illumination depth exponentially if the surface roughness effects on light irradiation are not considered (Qin et al., 2007). As the current densities J_n and J_p are the same at each point along the current path, the photocurrent may be expressed as:

$$i_{33} = \bar{k}_3 \alpha I_o e^{-\alpha H} \tag{11}$$

Eq. (11) is a simplified expression based on the formulation given in Qin et al. (2007), where $\bar{k}_3$ is referred to as the photocurrent coefficient, which depends on temperature, Boltzmann constant, electron–hole mobility and lifetime (Qin et al., 2007).

When near-violet light illuminates on surface of a PLZT wafer with 0-1 polarization, the induced field strength E_{11} is uniform along thickness direction because of the same electrical potential at the left or right electrode shown in Fig. 1(a). Therefore, the photo-induced strain in this type of PLZT wafer is uniformly distributed through the thickness. A comparison of formulas for the electrical performance and mechanical strains of PLZT actuators with 0-1 and 0-3 polarization is given in Table 2.

In Table 2, formulas for 0-1 polarized PLZT actuators are taken from Poosanaas-Burke et al. (1998), in which L_a and w_a are PLZT length and width. Due to light intensity attenuation with the light penetration depth by Beer's law, photocurrent density decreases with light penetration depth but the field strength is uniform through the thickness of a 0-1 polarized PLZT wafer, whilst in a 0-3 polarized PLZT wafer, photocurrent density is the same through the current path (thickness) but the field strength decreases with light penetration depth. It is noted that the photovoltaic voltage normally exceeds the energy gap (E_g) of PLZT materials by several orders of magnitude (Fridkin, 1979; Poosanaas-Burke et al., 1998).

2.3. Voltage source model, nonlinear features

In a process of electrical field generation caused by light illumination on PLZT materials, part of optical energy is converted to electrical energy. The photo-induced electrical field in a dielectric material has a nonlinear response, and the polarization is given by (Fridkin, 1979; Poosanaas-Burke et al., 2000):

$$P = \chi_o\left(\chi^{(1)} E_{op} \cos \omega_{op} t + \chi^{(2)} E_{op}^2 \cos^2 \omega_{op} t\right) \tag{12}$$

where ω_{op} is the light frequency; χ_o is a permittivity in vacuum; E_{op} is the photo-induced field strength; $\chi^{(1)}$ and $\chi^{(2)}$ are the 1st and 2nd order susceptibilities.

Table 1
Parameter values and references for PLZT 3/52/48.

d_{31} (m/V)	κ_d (Ω^{-1}m^{-1})	k_{ph} (Ω^{-1}m/W)	α (μm^{-1})	α_s
-154×10^{-12} [a]	8.8×10^{-10} [b]	6.3×10^{-12} [b]	2 [d]	0.60 [d]
	2.7×10^{-11} [c]	1.8×10^{-10} [c]	0.252 [e]	0.782 [e]

[a] Uchino et al. (1985)
[b] Ichiki et al. (2004).
[c] Nonaka et al. (1995).
[d] Qin et al. (2007).
[e] Poosanaas-Burke et al. (1998) for 0-1 polarized PLZT actuators.

Table 2
Photo-responsive features of PLZT wafers with 0-1 and 0-3 polarizations.

Polarization	Poling in 0-1 direction	Poling in 0-3 direction
Light intensity $I(z_d)$	$I_o e^{-\alpha z_d}$	$I_o e^{-\alpha z_d}$
Photocurrent density J_{ph}	$k_1 \alpha I_o e^{-\alpha z_d}$	$k_3 \alpha I_o e^{-\alpha z_d}$
Photocurrent i_{ph}	$i_{11} = k_1 I_o (1 - e^{-\alpha H})$	$i_{33} = \bar{k}_3 \alpha I_o e^{-\alpha H}$
Photo voltage V_{ph}	$V_{11} = \frac{L_a k_1 I_o (1 - e^{-\alpha H})}{w_a [\kappa_d H + \kappa_{ph} I_o (1 - e^{-\alpha H})/\alpha]}$	$V_{33} = \frac{k_3}{\kappa_{ph}} \ln \frac{\kappa_d + \kappa_{ph} I_o}{\kappa_d + \kappa_{ph} I_o e^{-\alpha H}}$
Electrical field strength	$E_{11} = \frac{k_1 I_o (1 - e^{-\alpha H})}{w_a [\kappa_d H + \kappa_{ph} I_o (1 - e^{-\alpha H})/\alpha]}$	$E_{33} = \frac{k_3 \alpha I_o e^{-\alpha z_d}}{\kappa_d + \kappa_{ph} I_o e^{-\alpha z_d}}$
Photo-induced strain	$\varepsilon_{ii} = d_{1i} E_{11}$ $(i = 1,2,3)$	$\varepsilon_{ii} = d_{3i} E_{33}$ $(i = 1,2,3)$

In dielectrics, a local electrical field is different from a macroscopic one as an additional field appears in polarized dielectrics due to the polarization charges. By using the Lorentz relation for ferroelectric materials, a local field in dielectrics can be expressed as (Fridkin, 1979; Poosanaas-Burke et al., 2000):

$$E_{loc} = E_{mac} + \frac{\gamma P}{3\chi_o} = E_{op}\cos\omega_{op}t + \frac{\gamma}{3}\left(\chi^{(1)}E_{op}\cos\omega_{op}t + \chi^{(2)}E_{op}^2\cos^2\omega_{op}t\right) \tag{13}$$

where E_{mac} is the macroscopic electrical field and γ is the Lorentz factor. The average local electrical field can be found by integrating equation (13) in one wavelength of light wave.

When coherent light illuminates a PLZT wafer with 0-1 polarization, the local average field strength E_{11} is given by (Fridkin, 1979; Poosanaas-Burke et al., 2000):

$$E_{11} = \overline{E}_{loc} = \frac{\gamma\chi_1^{(2)}}{6}E_{op}^2 = \frac{\gamma\chi_1^{(2)}}{6}I_{op} \tag{14}$$

where γ is the Lorentz factor; I_{op} is the light intensity; $\chi_1^{(2)}$ is the 2nd order susceptibility component in 0-1 direction.

The field strength induced in PLZT with 0-3 polarization can be obtained similarly as follows:

$$E_{33} = \overline{E}_{loc}(z_d) = \frac{\gamma\chi_3^{(2)}}{6}E_{op}^2(z_d) = \frac{\gamma\chi_3^{(2)}}{6}I_{op}(z_d) = \frac{\gamma\chi_3^{(2)}I_o}{6}e^{-\alpha z_d} \tag{15}$$

where $\chi_3^{(2)}$ the 2nd order susceptibility component in 0-3 direction. Eq. (15) is the photo-induced field strength derived using the linear voltage source model.

In order to achieve sufficiently photovoltaic field strength, strong light intensity is required and a high pressure mercury lamp is normally used (Poosanaas-Burke et al., 1998; Ichiki et al., 2004; Yao et al., 2005). When a high pressure mercury lamp is used as light source, incident light is incoherent. Incoherent light causes nonlinear photovoltaic effect and the effective field strength should be modified as (Fridkin, 1979; Poosanaas-Burke et al., 2000):

$$\overline{E}_{loc} = c_1\gamma\chi^{(2)}(E_{op}^2)^{\beta} \tag{16}$$

where c_1 is a constant and β is a parameter expressing the depression effect.

By replacing variable E_{op}^2 with light intensity I_{op} and considering the field strength variation through the thickness of a PLZT wafer with 0-3 polarization, the DC field strength at z_d and the electrical potential between the upper and lower electrodes can be obtained:

$$E_{33} = E_{dc} = c_2\gamma\chi_3^{(2)}(I_o)^{\beta}e^{-\bar{\alpha}z_d}; \quad V_{33} = \frac{c_2\gamma\chi_3^{(2)}(I_o)^{\beta}}{\bar{\alpha}}(1 - e^{-\bar{\alpha}H}) \tag{17}$$

In Eq. (17), $\bar{\alpha} = \alpha\beta$; c_2 is a constant; and E_{dc} is an effective DC field of photo-induced charge carriers. Eq. (17) denotes the photo-induced field strength and voltage based on the nonlinear voltage source model.

By comparing Eq. (15) with (10), exponential attenuation of photo-induced field strength and strain are obtained by the present simplified formulation and the linear voltage source model, and the photo-induced strain is linearly related to light intensity. By comparing Eq. (17) with Eqs. (6)–(8), nonlinearity of the photo-induced field strength and strain are reflected in the present model and the nonlinear voltage source model but the formulas given in Eqs. 17 and (6)–(8) are different. In the subsequent formulations, Eqs. (7)–(10) derived from the basic photovoltaic equations will be mainly used.

3. Constitutive equations of 0-3 polarized PLZT actuators

3.1. Energy transformation of light illumination on PLZT

The photostrictive phenomenon includes complicated processes of energy transformation (Fukuda et al., 1995; Shih and Tzou, 2000): (1) photovoltaic effect generating electrical field, (2) optothermic effect causing temperature increase, (3) pyroelectric effect producing electrical field due to heat, (4) converse piezoelectric effect inducing mechanical strain sourced by photovoltaic and pyroelectric fields, and (5) thermal expansion resulting in mechanical strain. Therefore, mechanical deformation induced by light illumination in PLZT materials includes piezoelectric and thermal strains.

When exposed to light, PLZT materials will be heated up by light irradiation. This process is called an optothermic effect, in which optical energy is partly converted to thermal energy that increases temperature of PLZT materials. The temperature increase results in thermal expansion, in which heat energy transfers into mechanical energy. The thermal strain $(\varepsilon_T)_{ii}$ in a PLZT wafer is given by:

$$(\varepsilon_T)_{ii} = (\alpha_T)_{ii}\Delta T \quad (i = 1,2,3) \tag{18}$$

where $(\alpha_T)_{ii}$ are thermal expansion coefficients and ΔT is a temperature increment. As PLZT ceramics are heat conductors, it can be assumed that temperature is the same within the PLZT material, and thus the thermal strain component is a constant in a PLZT wafers.

When temperature in the PLZT material increases to a specific point, an additional electrical field E_T will be triggered. In this process, thermal energy is converted to electric energy and it is referred to as pyroelectricity. The additional electrical field E_T can be defined as:

$$E_T = \left(\frac{P_n}{\chi_3^{(1)}}\right)T \quad (T \geqslant T_{trig.}) \tag{19}$$

where P_n is the pyroelectric constant; $\chi_3^{(1)}$ is the 1st order permittivity component in 0-3 direction; T is the temperature in a PLZT wafer and $T_{trig.}$ is a specific temperature to trigger the pyroelectric effect. It is noted that Eq. (19) is obtained for PLZT actuators with 0-3 polarization by using the definitions in Fukuda et al. (1995) and Shih and Tzou (2000) for PLZT actuators with 0-1 polarization.

Due to the converse piezoelectric effect, additional strain will be generated by the pyroelectric field strength E_T. Since the temperature in a heat conductor is the same, the electrical field E_T will not vary with light penetration depth and thus this stain is constant through the thickness. The heat triggers the pyroelectric effect and then enhances the photo-induced electrical field. However, heat interferes with photodeformation process, which reduces the photo effect when PLZT wafer's temperature becomes higher. By taking into consideration these effects, nonlinear constitutive equations will be developed in the subsequent section.

3.2. Nonlinear constitutive equations

As discussed in Section 3.1, the total strain in PLZT wafers with 0-3 polarization induced by light illumination can be expressed as:

$$\begin{aligned}\varepsilon_{ii} &= d_{3i}(E_{ph} + E_T) + (\alpha_T)_{ii}\Delta T \\ &= \frac{d_{3i}k_3\alpha I_o e^{-\alpha z_d}}{\kappa_d + \kappa_{ph}I_o e^{-\alpha z_d}} + \left(\frac{d_{3i}P_n}{\chi_3^{(1)}}T + (\alpha_T)_{ii}\Delta T\right) \quad (i = 1,2,3)\end{aligned} \tag{20}$$

Eq. (20) can be rewritten in the following compact form:

$$\varepsilon_{ii}(z_d) = \varepsilon_{oii}f(z_d) + (\varepsilon_T)_{ii} \quad (i = 1,2,3) \tag{21}$$

where

$$\varepsilon_{oii} = \frac{d_{3i}k_3\alpha I_o}{\kappa_d}; \quad f(z_d) = \frac{e^{-\alpha z_d}}{1 + (\kappa_{ph}I_o/\kappa_d)e^{-\alpha z_d}}$$
$$(\varepsilon_T)_{ii} = \frac{d_{3i}P_n}{\chi_3^{(1)}}T + (\alpha_T)_{ii}\Delta T \quad (i = 1,2,3) \tag{22}$$

Because only steady state is considered here, the time dependent strain and the voltage leakage influence (Fukuda et al., 1995; Shih and Tzou, 2000; Sun and Tong, 2007) are not involved. With an increase of illumination time, steady state will be reached and then photovoltaic field strength will become saturated.

By using Eq. (20), linear constitutive equations of 0-3 polarized PLZT ceramics are readily obtained. It has been known that ferroelectric ceramics exhibit increasingly nonlinear properties with stronger electrical field. Under strong light illumination, high field strength will be induced and thus nonlinear characteristics of PLZT materials should be considered (Dimos et al., 1994; Poosanaas-Burke et al., 2000; Ichiki et al., 2004). The nonlinearities of ferroelectric ceramics are described by a hysteresis loop of electrical polarization and a butterfly loop of mechanical strain.

To model a hysteresis loop of the electrical polarization and a butterfly loop of the mechanical strain of ferroelectric materials, three different methods have been used (Klinkel, 2006; Kim and Seelecke, 2007; Hegewald et al., 2008): a macro model based on thermodynamics, a micro-model based on micro-mechanics and a mathematical model containing some operators to describe the hysteresis loop of electrical polarization and the butterfly loop of mechanical strain.

In studying nonlinear properties of ferroelectric ceramics, an initial step taken by many researchers is to utilizing concepts of irreversible strain and polarization and then iterative algorithm is developed (Landis, 2004; Klinkel, 2006; Hegewald et al., 2008).

Dimos et al. (1994) discussed photo-induced hysteresis changes in PLZT thin films. Under strong light illumination, high filed strength E_{33} will be generated in 0-3 polarized PLZT ceramics. It is known that the high electric field in ferroelectric materials causes polarization switching and then the remanent polarization and strain develop. In light of investigations of Landis (2004), Klinkel (2006) and Hegewald et al. (2008), the polarization switching criterion of PLZT subjected to light illumination and mechanical loading can be expressed as:

$$\{\boldsymbol{\sigma}\}^T\{\Delta\boldsymbol{\varepsilon}\} + \{\boldsymbol{E}\}^T\{\Delta\boldsymbol{P}\} \geqslant 2P^sE_c \tag{23}$$

where $\{\Delta\boldsymbol{\varepsilon}\}$ and $\{\Delta\boldsymbol{P}\}$ are increments in strain and polarization during polarization switching; $P^s$is the spontaneous polarization; E_c is the coercive field strength. During polarization switching, the nonlinear constitutive equations for 0-3 polarized PLZT materials can be written as:

$$\begin{cases} \{\boldsymbol{\varepsilon}\} = [\boldsymbol{s}]\{\boldsymbol{\sigma}\} + \{\boldsymbol{\varepsilon}_T\} + [\boldsymbol{d}]\{\boldsymbol{E}\} + \{\boldsymbol{\varepsilon}^{\boldsymbol{r}}\} \\ \{\boldsymbol{D}\} = [\boldsymbol{d}]^T\{\boldsymbol{\sigma}\} + [\boldsymbol{\chi}]\{\boldsymbol{E}\} + \{\boldsymbol{P}^{\boldsymbol{r}}\} \end{cases} \tag{24}$$

where $\{\boldsymbol{\varepsilon}^{\boldsymbol{r}}\}$ and $\{\boldsymbol{P}^{\boldsymbol{r}}\}$are the macroscopic remanent strain and polarization, which are irreversible. In Eqs. (23) and (24), $\{\boldsymbol{\varepsilon}\}$ and $\{\boldsymbol{\sigma}\}$ are strain and stress vectors; $\{\boldsymbol{\varepsilon}_T\}(=\{\varepsilon_T,\varepsilon_T,\varepsilon_T,0,0,0\}^T)$ is the thermal strain vector; $\{\boldsymbol{E}\}(=\{0,0,E_{33}\}^T)$ is the field strength vector and E_{33} is given in Eq. (6); $\{\boldsymbol{D}\}(=\{0,0,D_{33}\}^T)$ is the electrical displacement vector; $[\boldsymbol{s}]$, $[\boldsymbol{d}]$ and $[\boldsymbol{\chi}]$ denote compliance, piezoelectric and dielectric permittivity.

In the subsequent section, we will present numerical results to verify the present model for the 0-3 polarized wafer expressed in Eqs. (8)–(11). Investigation into applications of the constitutive equations shown in Eq. (24) will be limited to the linear analysis in this paper as we lack data of the spontaneous polarization and the coercive strength for the 0-3 polarized PLZT ceramics.

4. Numerical results and model validation

4.1. Photovoltaic current

Qin et al. (2007) studied the effect of thickness on photocurrent of PLZT wafers with 0-3 polarization. They derived a photocurrent formula expressed in terms of wafer thickness by using the continuity equations of photocharge carriers, and then measured photocurrents of the PLZT wafers. By using the present formula in Eq. (11), photocurrent i_{33} can be calculated if $\bar{k}_3$ can be determined.

In the experiment conducted by Qin et al. (2007), the material was PLZT 3/52/48. Its light absorption coefficient and surface transmittance are $\alpha = 2\ \mu m^{-1}$ and $\alpha_s = 0.6$, respectively. In their experiment, Qin et al. (2007) reported nine values of the photocurrent corresponding to different thicknesses (0.26, 0.54 and 1.05 μm) and light intensities (0.22, 0.40 and 0.60 mW/cm^2). By using the experiment data in Fig. 5 of Qin et al. (2007), the photovoltaic coefficient $\bar{k}$ can be determined. In the present calculation, all nine experiment data in Fig. 5 of Qin et al. (2007) are used to calculate $\bar{k}_3$ and their average is adopted to calculate the photocurrent using Eq. (11).

Photocurrents versus PLZT wafer thickness predicted and measured by Qin et al. (2007) (data are taken from Fig. 5) and predicted by the present Eq. (11) are shown in Fig. 3(a),3(b),3(c). The numerical comparisons shown in Fig. 3(a),3(b),3(c) indicate that the photocurrent predicted by the present simplified formulation correlates well with those predicted and measured by Qin et al. (2007).

Ichiki et al. (2005) studied photovoltaic effect of PLZT wafers with 0-3 polarization. They measured photovoltaic current and voltage under light illumination with different intensities. In their experiment, the PLZT wafer size was $10.0 \times 10.0 \times 0.004$ mm^3 and the material was PLZT 3/52/48. The light absorption coefficient and the surface transmittance were not given in Ichiki et al. (2004, 2005). As the material composition (PLZT 3/52/48) in Ichiki et al. (2004, 2005) is the same as that in Qin et al. (2007), $\alpha = 2\ \mu m^{-1}$ and $\alpha_s = 0.6$ will be used in the present photocurrent calculation.

The nine data given in Fig. 6(a) of Ichiki et al. (2005) are used to calculate $\bar{k}_3$ and the average value of $\bar{k}_3$ is adopted in the prediction of the photocurrent. The photocurrents predicted by the present formula in Eq. (11) and measured by Ichiki et al. (2005) are plotted in Fig. 4. The observed good correlation validates Eq. (11). It is noted that Eq. (11) is a simplified equation from the formulation in Qin et al. (2007), and the photocurrent coefficient $\bar{k}_3$ in Eq.

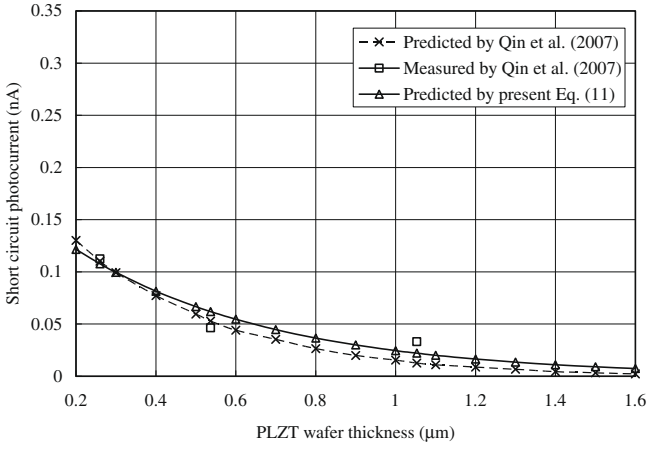

Fig. 3(a). Photovoltaic current vs. thickness predicted by Qin et al. (2007) and present Eq. (11) ($I_i = 0.22$ mW/cm^2).

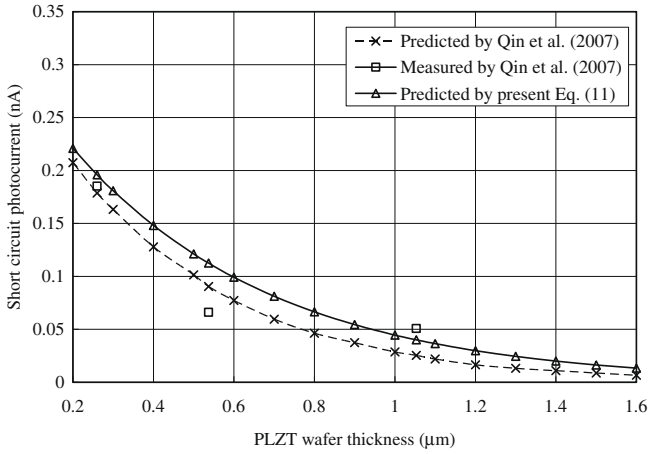

Fig. 3(b). Photovoltaic current vs. thickness predicted by Qin et al. (2007) and present Eq. (11) ($I_i = 0.40\ \mathrm{mW/cm^2}$).

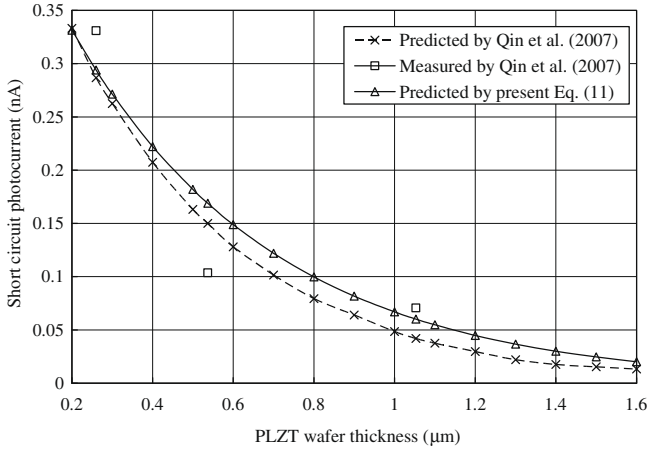

Fig. 3(c). Photovoltaic current vs. thickness predicted by Qin et al. (2007) and present Eq. (11) ($I_i = 0.60\ \mathrm{mW/cm^2}$).

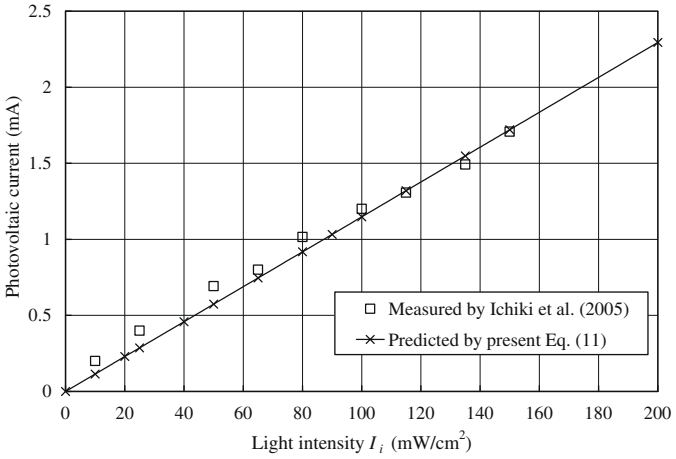

Fig. 4. Photovoltaic current measured by Ichiki et al. (2005) and predicted by present Eq. (11).

(11) is related to a number of factors such as temperature and electron–hole lifetime as indicated in Section 3. Ichiki et al. (2005) observed that the photocurrent was linearly proportional to the incident light intensity approximately. This fact is also supported by Eq. (11) and Fig. 4.

4.2. Photovoltaic voltage

The nonlinearity in the relationship between photovoltaic voltage and light intensity can be seen from Fig. 6(b) in Ichiki et al. (2005). To verify Eq. (9), we use Eq. (8) to calculate photovoltaic voltage in a PLZT wafer with 0-3 polarization and then compare with the experimental data reported in Ichiki et al. (2005).

To calculate the photovaltage using Eq. (8), we need to determine the relevant parameters. Ichiki et al. (2004) measured dark and photo conductivities of PLZT 3/52/48: $\kappa_d = 8.8 \times 10^{-10}$ S/m and $\kappa_{ph} = 6.3 \times 10^{-12}\ \Omega\mathrm{m/W}$. As the same material was used in Ichiki et al. (2004) and Ichiki et al. (2005), these values will be used here. Also, $\alpha = 2\ \mu\mathrm{m}^{-1}$ and $\alpha_s = 0.6$ are used in the present photovoltaic prediction.

The photocurrent density coefficient k_3 can be calibrated using the experimental data in Ichiki et al. (2005). The nine data in Fig. 6(b) of Ichiki et al. (2005) and Eq. (8) are used to calculate k_3 and its average value, as listed in Table 3. By referring to Table 3, k_3 at $I_i = 10\ \mathrm{mW/cm^2}$ is obviously larger than that corresponding to other light intensities. This datum is still used in the average to have a comparison with all experimental data as light illumination on PLZT materials involves a complex energy transformation process as discussed in Fukuda et al. (1995) and Shih and Tzou (2000). The photovoltaic voltages predicted by Eq. (8) and measured by Ichiki et al. (2005) are illustrated in Fig. 5; it indicates that the present Eq. (8) can be used to predict approximately the photovoltaic voltage.

The photo voltage predicted by Eq. (17) is also given in Fig. 5. In the present calculation, the photo voltage in Eq. (17) is rewritten as: $V_{33} = k_{3V}(I_o)^{\beta}(1 - e^{-\bar{\alpha}H})$. The depression coefficient was given in Poosanaas-Burke et al. (2000) for PLZT 3/52/48 with 0-1 polarization: $\beta = 0.46$. It is assumed this value is valid for the PLZT 3/52/48 with 0-3 polarization. Also, the 9 measured data reported in Ichiki et al. (2005) are used to calculate k_{3V} and the average is used to predict the photovoltaic voltage. Fig. 5 shows that the voltage predicted by Eq. (17) based on the nonlinear voltage source model correlates with the measured data (Ichiki et al., 2005) slightly better than that predicted by Eq. (8) derived from the basic photovoltaic equations.

In Fig. 5, the photovoltaic voltage predicted by Eq. (10) is given in a range of 0—30 mW/cm^2, in which k_3 is calibrated using the voltage at $I_i = 25\ \mathrm{mW/cm^2}$. Fig. 5 indicates that the simplified formulation in Eq. (10) is applicable for low light intensity, e.g., $I_i < 20\ \mathrm{mW/cm^2}$. It is noted that $I_i > 20\ \mathrm{mW/cm^2}$ represents very strong light illumination according to the experiments conducted by Poosanaas-Burke et al. (1998, 2000), Ichiki et al. (2004, 2005), Yao et al. (2005) and Qin et al. (2007).

The light absorption coefficient is an important parameter in studying light transmission in solid. $\alpha = 0.0252\ \mu\mathrm{m}^{-1}$ and $\alpha = 2\ \mu\mathrm{m}^{-1}$ are given in Poosanaas-Burke et al. (1998) for the 0-1 polarization and in Qin et al. (2007) for the 0-3 polarization, respectively. In the measurement in Ichiki et al. (2004, 2005), the light absorption coefficient was not involved. Fig. 6 illustrates the photovoltaic voltage predicted by the present formula in Eq. (8) by using different α values to further verify the present formulation.

Figs. 5 and 6 confirm the validity of Eq. (8). It is noted that Eqs. (8) and (9) are derived from Eq. (6), and only equations of an electrical field and converse piezoelectricity are used in the derivation. Therefore, the photo-induced strain given in Eq. (9) reasonably captures basic mechanical performance of 0-3 polarized PLZT actuators subjected to light illumination.

Table 3
Calculation of the photocurrent density coefficient k_3.

I_i (mW/cm^2)	10	25	50	65	80	100	115	135	150	
$k_3(\times 10^{-12})$	6.81	4.12	3.29	3.15	3.05	3.01	2.87	2.74	2.71	3.53 (Average)

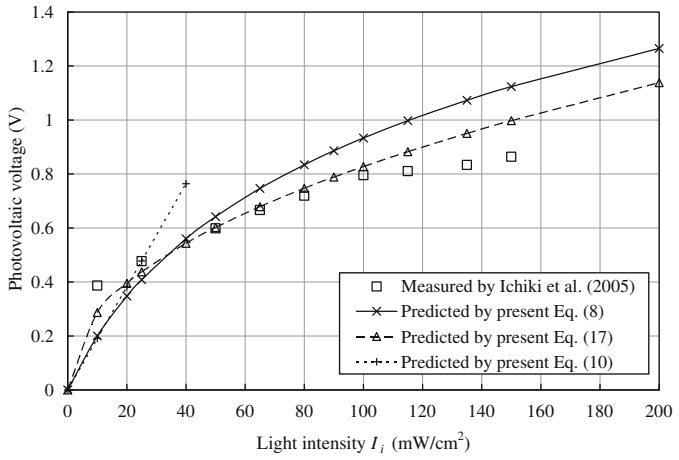

Fig. 5. Photovoltaic voltage measured by Ichiki et al. (2005) and predicted by the present formulations.

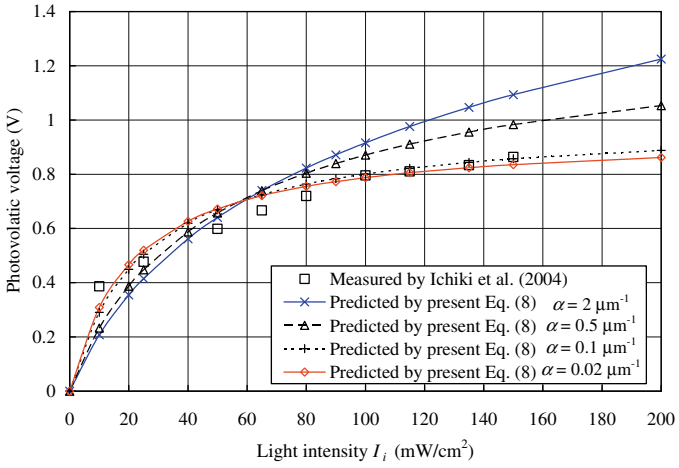

Fig. 6. Photovoltaic voltage measured by Ichiki et al. (2005) and predicted by present Eq. (8) for different values of the light absorption coefficient.

4.3. Applications of PLZT actuators in intelligent structures

Since the photo-induced strain in a PLZT wafer with 0-3 polarization varies with light penetration depth, it can be used as a unimorph or photocantilever. When this material is deposited on a substrate, this layered beam driven by light illumination can be used as a bimorph. When PLZT wafers are mounted on a host beam, they can be used actuators in an intelligent beam structure. These configurations have been widely used in MEMS/MOMS and intelligent structures. Therefore, their formulations have important applications and the closed form solutions will be given here.

As shown in Fig. 7(a), the stress–strain relation in linear analysis can be written as:

$$\sigma_x(z) = E'[\varepsilon_x(z) - \varepsilon_T - \varepsilon_o f(z)] \text{ where } f(z) = \frac{e^{-\alpha(H/2-z)}}{1 + (\kappa_{ph} I_o/\kappa_d)e^{-\alpha(H/2-z)}} \tag{25}$$

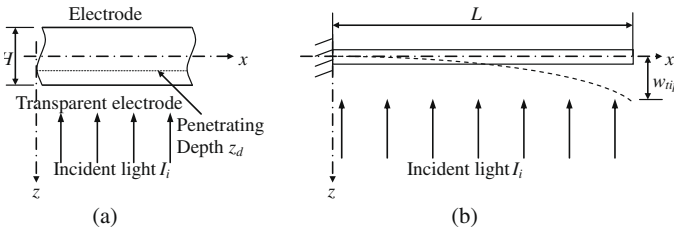

Fig. 7. (a) Light illumination on surface of a PLZT wafer with 0-3 polarization and (b) a unimorph driven by light illumination.

in which σ_x is the normal stress along axis x; E' is the effective elastic modulus. $E' = E$ for plane stress state and $E' = E/(1-\nu^2)$ for plane strain state, where E and ν are Young's modulus and Poisson's ratio. When the classical beam theory is used to model a unimorph in Fig. 7(b), axial force N and bending moment M in the unimorph cross-section are:

$$\begin{cases} N = E'H(\varepsilon_c - \varepsilon_T) - \dfrac{E'\varepsilon_o\kappa_d}{\alpha\kappa_{ph}I_o}\ln\dfrac{\kappa_d + \kappa_{ph}I_o}{\kappa_d + \kappa_{ph}I_o e^{-\alpha H}} \\ M = -\frac{D}{\rho_c} - E'\varepsilon_c\int_{-H/2}^{H/2} f(z)z\,dz \end{cases} \tag{26}$$

where D is the bending stiffness; H is the height of the unimorph. It is noted that the unit width has been assumed in Eq. (26) and this assumption will also be used in the subsequent discussions. The integration on $f(z)z$ results in a polylogarithmic function, which is not expanded in Eq. (26) to have a clear expression.

By using Eq. (26), strain ε_c and curvature $(1/\rho_c)$ can be solved when there is no mechanical loading. After the curvature is found, the tip deflection, a primary parameter of a unimorph under light illumination, is readily obtained.

In a bimorph of Fig. 8(a), temperature in an inactive layer may also increase under light illumination. Strain ε_h in an inactive layer caused by thermal expansion is normally unequal to the thermal strain ε_T in a PLZT layer due to the difference in thermal expansion coefficients. The stress–strain relationship for a bimorph of Fig. 8(a) can be written as:

$$\sigma_x = \begin{cases} E'_h[(\varepsilon_c - \varepsilon_h) - z/\rho_c] & -(t_h + t_p)/2 \leqslant z < (t_h - t_p)/2 \\ E'_p[(\varepsilon_c - \varepsilon_T) - z/\rho_c - \varepsilon_o f(z)] & (t_h - t_p)/2 \leqslant z < (t_h + t_p)/2 \end{cases} \tag{27}$$

where t_p and t_h are thicknesses of PLZT and inactive layers; E'_p and E'_h are their effective elastic moduli; and ε_h is the thermal strain

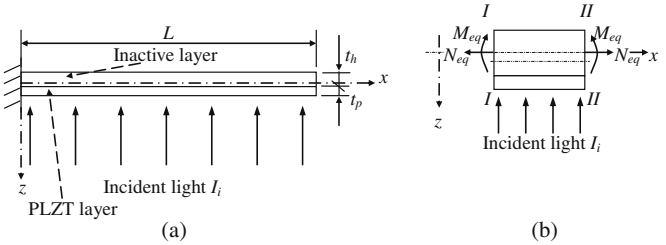

Fig. 8. (a) Bimorph driven by light illumination and (b) equivalent force components in a host beam mounted with the PLZT photo-actuator.

caused by temperature variation in an inactive layer. Using Eq. (27), one has:

$$\begin{cases} N=\left(E_h't_h+E_p't_p\right)\varepsilon_c-\frac{1}{\rho_c}\left(E_h'S_h+E_p'S_p\right)-E_h't_h\varepsilon_h-E_p't_p\varepsilon_p-\dfrac{E'\varepsilon_o\kappa_d}{\alpha\kappa_{ph}I_o}\ln\dfrac{\kappa_d+\kappa_{ph}I_o}{\kappa_d+\kappa_{ph}I_oe^{-\alpha t_p}} \\ M=\left(E_h'S_h+E_p'S_p\right)\varepsilon_c-\frac{1}{\rho_c}\left(E_h'I_h+E_p'I_p\right)-E_h'S_h\varepsilon_h-E_p'S_p\varepsilon_p-E'\varepsilon_c\int_{(t_h-t_p)/2}^{(t_h-t_p)/2}f(z)z\,dz \end{cases} \tag{28}$$

where, S_h and S_p are area moments with respect to the mid-plane; I_h and I_p are the inertial moments; subscripts h and p represent the host layer and the PLZT respectively. When there is no applied force, the photo-induced train, curvature and tip-deflection of the bimorph are solved from Eq. (28).

A host beam with bonded actuators and sensors has been widely adopted as an important configuration in intelligent structural systems. When the host beam is mounted with PLZT wafers with 0-1 polarization, the induced strain is uniformly distributed through the thickness of PLZT. The host beam with this type of actuation is similar to the PZT based intelligent beam, which have been extensively studied in the past decades. In the host beam mounted with PLZT actuators with 0-3 polarization, the photo-induced strain varies with light penetration depth. In this case, the stress–strain relationship is the same as that in Eq. (27).

It is assumed the host beam and the PLZT patch are perfectly joined and the interface is sufficiently thin and can be ignored. Fig. 8(a) illustrates a host beam mounted with a PLZT actuator with 0-3 polarization, the equivalent forces activated at cross-sections I-I and II-II of the host beam by light illumination are of importance and their formulations are given below.

Referring to Fig. 8(b) and using the constitutive equations based on the classical beam theory, we have:

$$\varepsilon_{hc}=\varepsilon_c+\frac{t_p}{2\rho_c};\quad N_{eq}=E_h't_h\varepsilon_{hc};\quad M_{eq}=-\frac{E_h'I_{hc}}{\rho_c-t_p/2}\approx-\frac{E_h'I_{hc}}{\rho_c};\quad I_{hc}=\frac{t_h^3}{12} \tag{29}$$

When there is no mechanical force, the following equilibrium equations can be derived by utilizing Eqs. (27) and (29):

$$\begin{cases} (1+r_t\psi)N_{eq}+\dfrac{6r_t\psi(1+r_t)}{t_h}M_{eq}-E_h't_h\varepsilon_h-E_p't_p\varepsilon_T+N_{ph}=0 \\ \frac{t_p}{2}(\psi-1)N_{eq}+(1+3r_t\psi+3r_t^2\psi+r_t^3\psi)M_{eq}-E_h't_h\varepsilon_h-E_p't_p\varepsilon_T+M_{ph}=0 \end{cases} \tag{30}$$

where

$$r_t=\frac{t_p}{t_h};\quad \psi=\frac{E_p'}{E_h'};\quad N_{ph}=-\frac{E'\varepsilon_o\kappa_d}{\alpha\kappa_{ph}I_o}\ln\frac{\kappa_d+\kappa_{ph}I_o}{\kappa_d+\kappa_{ph}I_oe^{-\alpha t_p}};\quad M_{ph}=-E'\varepsilon_c\int_{(t_h-t_p)/2}^{(t_h-t_p)/2}f(z)z\,dz \tag{31}$$

The equivalent force components N_{eq} and M_{eq} can then be solved from Eq. (31).

It is readily shown that, when the simplified photo-strain in Eq. (10) is used, tip deflection of the unimorph found via Eq. (26) correlates with that derived by Guo et al. (2007) for the silicon microcantilever. As Eq. (27) can be applied to a PLZT bimorph and a host beam with PLZT actuators, we only present the numerical comparison for the cantilever beam with the bonded PLZT patch.

Shih et al. (2005) discussed displacement control of a beam using optical actuators. The used optical actuators were 0-1 polarized PLZT wafers. In this type of PLZT actuators, the stress–strain relation is:

$$\sigma_x=\begin{cases} E_h'\left(\varepsilon_c-\frac{z}{\rho_c}\right) & -\frac{t_h+t_p}{2}\leqslant z<\frac{t_h-t_p}{2} \\ E_p'\left(\varepsilon_c-\frac{z}{\rho_c}-\varepsilon_s\right) & \frac{t_h-t_p}{2}\leqslant z<\frac{t_h+t_p}{2} \end{cases} \tag{32}$$

where ε_s is the photo induced strain in a PLZT actuator and it is defined as (Shih et al., 2005):

$$\varepsilon_s=d_{11}(\overline{E}_{ph}+E_T)+\alpha_T\Delta T \tag{33}$$

where $\overline{E}_{ph}$ and E_T is the photovoltaic field strength and the filed strength E_T is due to the pyroelectric effect.

Fig. 9 is a cantilever beam mounted with a PLZT actuator used in Shih et al. (2005). They calculated deflections of the host beam using finite element analysis (FEA) and an analytical method. In the analytical analysis, they derived the equivalent bending moment M_{eq} and then used the classic beam theory to calculate beam deflections. The derived M_{eq} was:

$$M_{eq}=\frac{t_h+t_p}{2}t_pE_p'\varepsilon_s=\frac{(1+r_t)t_ht_pE_p'\varepsilon_s}{2} \tag{34}$$

The cantilever deflections predicted by Shih et al. (2005) are shown in Fig. 10, in which the data are taken from Fig. 6 in Shih et al. (2005). Plane stress was considered in Shih et al. (2005); hence $E_h'=E_h$ and $E_p'=E_p$. Details of the input data can be referred to Shih et al. (2005) and those used in the present calculation are: $E_p=6.3\times10^{10}$ N/m^2, $E_h=2.1\times10^{11}$ N/m^2, $t_h=2$ mm, $l_a=0.1$ m, $c=0.2$ m, $L=1.0$ m; the PLZT actuator size: $200\times30\times0.3$ mm^3. In light of the input data in Shih et al. (2005), the photo-induced strain is: $\varepsilon_s=130.4\,\mu\varepsilon$.

The present formulation of the equivalent bending moment for this case can be obtained from Eq. (30), which is given by:

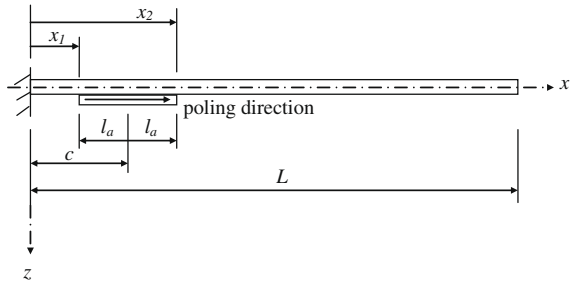

Fig. 9. Schematics of the cantilever with surface mounted with a PLZT actuator.

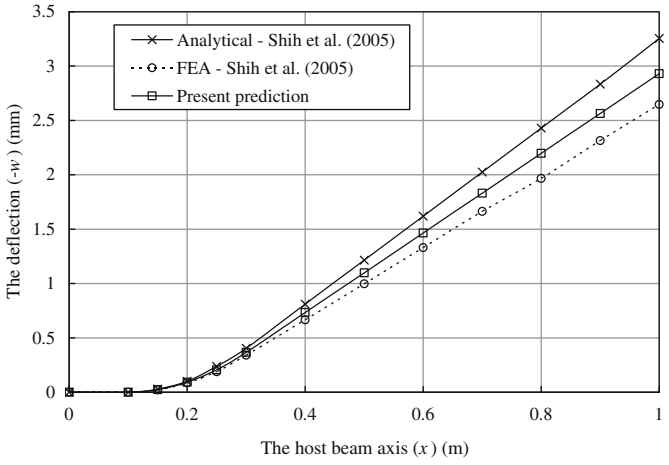

Fig. 10. The photo-induced deflection of the cantilever predicted by Shih et al. (2005) (analytical formulation and FEA) and the present formulation.

$$M_{eq} = \frac{(1+r_t)E'_p t_p t_h \varepsilon_s}{2[(1-r_t^2\psi)^2 + 4r_t\psi(1+r_t)^2]} \tag{35}$$

which is different from Eq. (34) derived by Shih et al. (2005).

The deflection of a cantilever in Fig. 9 can be calculated when the equivalent bending moment is determined. The deflection predicted by the present formulation is illustrated in Fig. 10. It is seen from Fig. 10 that the deflection predicted by the present solution correlates well with the FEA results in Shih et al. (2005).

5. Conclusion

The photo-induced electrical field strength in Eq. (6) is derived from the basic photovoltaic equations for 0-3 polarized PLZT actuators. Novel formulation of the photo-induced strain in Eq. (9) is obtained by superposing the photovoltaic and the converse piezoelectric effects. The features of the photo-induced strain in 0-3 polarized PLZT actuators are investigated. The photovoltaic voltage and current are also formulated and validated by comparing with experimental data in the literature. These comparisons confirm the present formulations for the photo-induced electrical field strength and strain.

On the basis of the new formulation of the photo-induced strain in PLZT actuators with 0-3 polarization, linear and nonlinear constitutive equations are developed. For the case of linear constitutive equations, analytical analyses for a unimorph, bimorph and host beam mounted PLZT actuators are presented; the closed-form solutions of tip deflections for a unimorph and bimorph and equivalent forces for an intelligent beam are obtained. The numerical results show that the present analytical solutions for an intelligent beam are valid and accurate.

Acknowledgments

The authors are grateful for the support of Australian Research Council via Discovery-Projects grants (DP0774596).

References

Brody, P.S., 1983. Optomechanical bimorph actuator. Ferroelectrics 50 (1–4), 27–32.
Camacho-Lopez, M., Finkelmann, H., Palffy-Muhoray, P., Shelley, M., 2004. Fast liquid-crystal elastomer swims into the dark. Nature Materials 3 (5), 307–310.
Charra, F., Kaizar, F., Nunzi, J.M., Raimond, P., Idiart, E., 1993. Light-induced 2nd harmonic generation in azo-dye. Optics Letters 18 (12), 941–943.
Dimos, D., Warren, W.L., Sinclair, M.B., Tuttle, B.A., Schwartz, R.W., 1994. Photoinduced hysteresis changes and optical storage in (Pb,La)(Zr,Ti)O_3 thin films and ceramics. Journal of Applied Physics 76 (7), 4305–4315.
Eisenbach, C.D., 1980. Isomerization of aromatic azo chromophores on poly (ethylacrylate) networks and photomechanical effect. Polymer 21 (10), 1175–1179.
Figielski, T., 1961. Photostriction effect in germanium. Physica Status Solidi 1 (4), 306–316.
Fridkin, V.M., 1979. Photoferroelectrics. Springer Series in Solid-state Sciences, vol. 9. Springer-Verlag Berlin, Heidelberg, New York.
Fridkin, V.M., Efremova, E.P., Karimov, B.H., Kuznezov, V.A., Kuzmina, I.P., LObachev, A.N., Lazarev, V.G., Rodin, A.J., 1981. The experimental investigation of the photovoltaic effect in some crystals without a center of symmetry. Applied Physics A: Materials Science and Processing 25 (1), 77–80.
Fukuda, T., Hattori, S., Arai, F., Nakamura, H., 1995. Performance improvement of optical actuator by double side irradiation. IEEE Transactions on Industrial Electronics 42 (5), 455–461.
Gauster, W.B., Habing, D.H., 1967. Electronic volume effect in silicon. Physical Review Letters 18 (24), 1058–1061.
Guo, Y.L., Zhou, J., Huang, Y.P., Bao, M.H., 2007. Modeling of photoinduced deformation in silicon microcantilevers. Sensors 7 (9), 1713–1719.
Hegewald, T., Kaltenbacher, B., Kaltenbacher, M., Lerch, R., 2008. Efficient modeling of ferroelectric behavior for the analysis of piezoceramic actuators. Journal of Intelligent Material Systems and Structures 19 (10), 1117–1129.
Ichiki, M., Morikawa, Y., Mabune, Y., Nakada, T., 2004. Electrical properties of photovoltaic lead lanthanum zirconate titanate in an electrostatic-optical motor application. Journal of the European Ceramic Society 24 (6), 1709–1714.
Ichiki, M., Morikawa, Y., Mabune, Y., Nakada, T., Nonaka, K., Maeda, R., 2005. Preparation of ferroelectric ceramics in a film structure and their photovoltaic properties. Microsystem Technologies 12 (1–2), 143–148.
Kim, S.J., Seelecke, S., 2007. A rate-dependent three-dimensional free energy model for ferroelectric single crystals. International Journal of Solids and Structures 44 (3–4), 1196–1209.
Klinkel, S., 2006. A phenomenological constitutive model for ferroelastic and ferroelectric hysteresis effects in ferroelectric ceramics. International Journal of Solids and Structures 43 (22–23), 7197–7222.
Landis, C.M., 2004. Non-linear constitutive modeling of ferroelectrics. Current Opinion in Solid State and Materials Science 8 (1), 59–69.
Leng, W.J., Yang, C.R., Ji, H., Zhang, J.H., Chen, H.W., Tang, J.L., 2006. Structure-related optical properties of (Pb,La)(Zr,Ti)O_3 thin films on indium tin oxide/quartz substrates. Journal of Applied Physics 100 (8). 083505-1-083505-6.
Luo, Q.T., Tong, L.Y., 2009. Constitutive modeling of photostrictive materials and design optimization of microcantilevers. Journal of Intelligent Material Systems and Structures 20 (12), 1425–1438.
Nonaka, K., Akiyama, M., Hagio, T., Takase, A., 1995. Bulk photovoltaic effect in reduced/oxidized lead lanthanum titanate zirconate ceramics. Japanese Journal of Applied Physics Part 1-Regular Papers Short Notes and Review Papers 34 (5A), 2344–2349.
Piprek, J., 2003. Semiconductor Optoelectronic Devices: Introduction to Physics and Simulation. Academic Press, Amsterdam, Boston.
Poosanaas-Burke, P., Dogan, A., Thakoor, S., Uchino, K., 1998. Influence of sample thickness on the performance of photostrictive ceramics. Journal of Applied Physics 84 (3), 1508–1512.
Poosanaas-Burke, P., Tonooka, K., Uchino, K., 2000. Photostrictive actuators. Mechatronics 10 (4–5), 467–487.
Qin, M., Yao, K., Shannigrahi, S., 2007. Thickness effects on photoinduced current in ferroelectric (Pb0.97 La0.03) (Zr0.52 Ti0.48) O_3 thin films. Journal of Applied Physics 101 (1). pp. 014104-1–014104-8.
Resta, R., Vanderbilt, D., 2007. Theory of polarization: a modern approach. In: Rabe, C.H., Ahn, J.M.T. (Eds.), Physics of Ferroelectrics: A Modern Perspective, vol. 105. Springer-Verlag, Berlin Heidelberg, pp. 31–68.
Saslow, W.M., 2002. Electricity, Magnetism, and Light. Academic Press, Amsterdam, Boston.
Shih, H.R., Tzou, H.S., 2000. Opto-piezothermoelastic constitutive modeling of a new 2-D photostrictive composite plate actuator. In: Tzou, H.S., Golnaraghi, M.F., Radcliffe, C.J. (Eds.), Proceedings of 2000 ASME International Mechanical Engineering Congress and Exposition, vol. 61. American Society of Mechanical Engineers, New York, pp. 1–8.
Shih, H.R., Watkins, J., Tzou, H.S., 2005. Displacement control of a beam using photostrictive optical actuators. Journal of Intelligent Material Systems and Structures 16 (4), 355–363.
Sun, D.C., Tong, L.Y., 2007. Modeling of wireless remote shape control for beams using nonlinear photostrictive actuators. International Journal of Solids and Structures 44 (2), 672–684.
Uchino, K., Aizawa, M., Numora, S., 1985. Photostrictive effect in (PbLa)(ZrTi)O_3. Ferroelectrics 64 (1–3), 199–208.
Warner, M., Mahadevan, L., 2004. Photoinduced deformations of beams, plates, and films. Physical Review Letters 92 (13). pp. 134302-1–134302-4.
Yao, K., Gan, B.K., Chen, M., Shannigrahi, S., 2005. Large photo-induced voltage in a ferroelectric thin film with in-plane polarization. Applied Physics Letters 87 (21). pp. 212906-1–212906-3.
Yu, Y., Nakano, M., Ikeda, T., 2003. Directed bending of a polymer film by light. Nature 425 (6954), 145.